EurJIC
European Journal of Inorganic Chemistry

Chemistry Europe
European Chemical Societies Publishing

Accepted Article

Title: Enhanced microwave dielectric properties in Mg2Al4Si5O18 through Cu2+ substitution

Authors: Fanshuo Wang, Yuanming Lai, Yiming Zeng, Fan Yang, Baoyang Li, Xizhi Yang, Hua Su, Jiao Han, and Xiaoling Zhong

To be cited as: *Eur. J. Inorg. Chem.* 10.1002/ejic.202100174

Link to VoR: https://doi.org/10.1002/ejic.202100174

WILEY-VCH

FULL PAPER WILEY-VCH

Enhanced microwave dielectric properties in $Mg_2Al_4Si_5O_{18}$ through Cu^{2+} substitution

Fanshuo Wang[a], Yuanming Lai*[a], Yiming Zeng*[b], Fan Yang[a], Baoyang Li[a], Xizhi Yang[a], Hua Su[c], Jiao Han[b], Xiaoling Zhong[a]

[a] Fanshuo Wang, Dr. Yuanming Lai, Fan Yang, Baoyang Li, Xizhi Yang, Prof. Xiaoling Zhong, *College of Information Science & Technology, Chengdu University of Technology, Chengdu 610059, China*
E-mail: laiyuanming19@cdut.edu.cn (Yuanming Lai)
[b] Dr. Yiming Zeng, Jiao Han, *State Key Laboratory of Advanced Technologies for Comprehensive Utilization of Platinum Metals, Kunming Institute of Precious Metals, Kunming 650106, China*
E-mail: zengym0871@126.com (Yiming Zeng)
[c] Prof.Dr. Hua Su, *State Key Laboratory of Electronic Thin Films and Integrated Devices, University of Electronic Science and Technology of China, Chengdu 610054, China*

Supporting information for this article is given via a link at the end of the document.

Abstract: The $Mg_2Al_4Si_5O_{18}$ ceramics are considered as a kind of important candidates for millimeter-wave applications. In this work, $Mg_{2-x}Cu_xAl_4Si_5O_{18}$ ($0 \le x \le 0.16$) ceramics were synthesized by solid-state reaction, aiming to improve the microwave dielectric properties. According to the XRD analysis, Cu^{2+} ions enter into the $Mg_2Al_4Si_5O_{18}$ lattice and form a solid solution. The dense microstructures were observed in the Cu-substituted $Mg_2Al_4Si_5O_{18}$ ceramics at x = 0.04 sintered at 1420 ℃ . The dielectric constant (ε_r) values depend on the microstructure, secondary phase and ionic polarizability of the samples. The quality factor (Qf) values are dominated by the microstructure, secondary phase and centro-symmetry of [Si_4Al_2] hexagonal ring. The temperature coefficients of resonance frequency (τ_f) are strongly related to the Mg/Cu-O bond valance. In comparison to pure $Mg_2Al_4Si_5O_{18}$ ceramics, the excellent microwave dielectric properties with ε_r = 4.56, Qf = 31,100 GHz and τ_f = −52 ppm/°C were obtained at x = 0.04 with sintering at 1420 ℃ . Thus, the $Mg_{2-x}Cu_xAl_4Si_5O_{18}$ ($0 \le x \le 0.16$) ceramics will be promising millimeter-wave communication materials.

Introduction

In recent years, the microwave dielectric ceramics are indispensable materials in millimeter-wave and even extending to THz band systems. The microwave dielectric materials can be used in many fields, such as antennas, duplexers, resonators and filters[1–3]. High performance materials for millimeter wave communication should have a low dielectric constant (ε_r), high quality factor (Qf), near zero temperature coefficient of resonance frequency (τ_f) and relatively low sintering temperature[4–7]. The low ε_r value can reduce the signal delay, high Qf value can achieve the better selectivity, and the near-zero τ_f value can improve stability[8–10].

Cordierite with low ε_r value (~5)[11], which is one of the ideal materials for millimeter-wave application, derives from silica tetrahedron with about 55% covalent bonding composed[12]. In general, the cordierite has two modifications, α-cordierite (indialite) and β-cordierite (cordierite), respectively. The α-cordierite (p6/mcc no.192), which was synthesized at high-temperature (1550-1600 ℃), is high symmetry hexagonal phase with disordered [$(Si,Al)O_4$] tetrahedrons arranging nearly equilateral hexagonal rings. The β-cordierite (Cccm no.66), which was synthesized at low temperature (1350-1475 ℃), is low symmetry orthorhombic phase with [$(Si,Al)O_4$] tetrahedrons arranging orderly [13,14]. However, the $Mg_2Al_4Si_5O_{18}$ ceramics with low densification and low Qf values do not satisfy the practical application of millimeter-wave communication. The high Qf value (~99,110 GHz) was achieved through the Ni^{2+} doping $Mg_2Al_4Si_5O_{18}$ ceramics, whereas increase of the ε_r value (~6.2) resulted in a longer signal delay time[12]. The $Mg_2Al_4Si_5O_{18}$ ceramics with substitution of Li^+ and Ga^{3+} for Mg^{2+} have the optimized Qf value (~42,170 GHz) and ε_r value (~4.72)[15]. But the Ga_2O_3 as starting material increase cost, which severely limits its commercial application, and its Qf value was deteriorated. The zero-near τ_f value of $Mg_2Al_4Si_5O_{18}$ ceramics was also investigated through adding $CaTiO_3$, TiO_2 and $SrTiO_3$[16–18]. Although the zero-near τ_f values were obtained, the ε_r values increased. In addition, the low temperature sintering of $Mg_2Al_4Si_5O_{18}$ ceramic was realized by adding $BaCu(B_2O_5)$ ceramics, whereas the Qf value was deteriorated[19]. The sintering temperature of $Mg_2Al_4Si_5O_{18}$ ceramics with Mg_2SiO_4 addition was reduced, while the ε_r value increased[20]

Furthermore, CuO, which served as sintering aid due to its low melt point of 1086 ℃ [6], was added to $(Zr_{0.8},Sn_{0.2})TiO_4$[21], $ZnNb_2O_6$[22], $Mg(Zr_{0.05}Ti_{0.95})O_3$[23], $0.95Ba(Zn_{1/3}Nb_{2/3})O_3$–$0.05BaZrO_3$[24], Mg_2SiO_4[25], Zn_2SiO_4[26] and $CaMgSi_2O_6$[27]. The Cu^{2+} (0.73 Å) ionic and Mg^{2+} (0.72 Å) ionic have similar ionic radius and same octahedral coordination. Therefore, the CuO can be added to Mg-based microwave dielectric ceramics to reduce the sintering temperature and improve the microwave dielectric properties.

In this work, CuO was added to the $Mg_2Al_4Si_5O_{18}$ ceramics in order to acquire low ε_r and high Qf value. $Mg_{2-x}Cu_xAl_4Si_5O_{18}$ ($0 \le x \le 0.16$) ceramics were prepared by solid-state method. The effects of CuO addition on the phase composition, microstructure and microwave dielectric properties of $Mg_2Al_4Si_5O_{18}$ ceramics were analyzed.

Results and Discussion

Figure. 1 shows the XRD patterns of the $Mg_{2-x}Cu_xAl_4Si_5O_{18}$ ($0 \le x \le 0.16$) ceramics sintered at 1420 ℃ for 4 h. All of the XRD patterns of samples show β-cordierite $Mg_2Al_4Si_5O_{18}$ (PDF #89-1487) as a major phase. Additionally, minor secondary phase of spinel $MgAl_2O_4$ was found at $x \le 0.08$, whereas the $MgAl_2O_4$ disappeared and the sillimanite mineral Al_2SiO_5 was detected at $x \ge 0.12$. The influence of the secondary phase about the microwave dielectric properties would be discussed in detail

below. In addition, it was clear that no phase containing Cu^{2+} ions was observed.

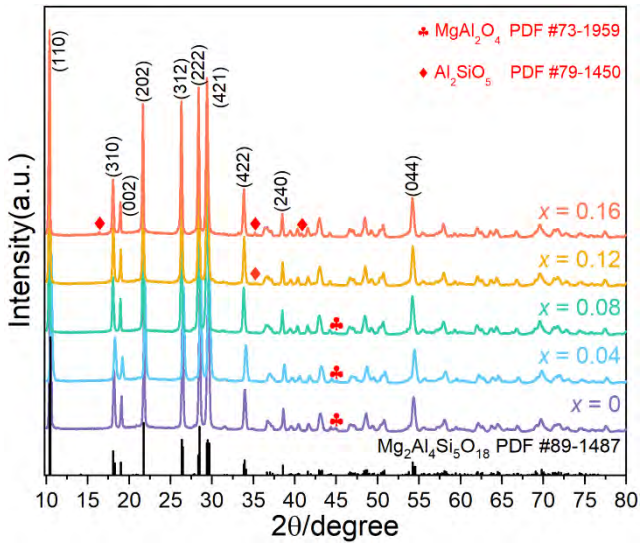

Figure 1. The XRD patterns for the $Mg_{2-x}Cu_xAl_4Si_5O_{18}$ ($0 \le x \le 0.16$) ceramics sintered at 1420 ℃

To further analyze the crystal structure, the FullProf software was carried out to refine the XRD data[28]. The $Mg_2Al_4Si_5O_{18}$ crystal has an orthorhombic structure with Cccm space group. **Table. 1** summarizes the lattice parameters of $Mg_{2-x}Cu_xAl_4Si_5O_{18}$ ($0 \le x \le 0.16$) ceramics, and **Figure. 2** shows the refined XRD patterns with $x = 0$ and $x = 0.04$ (Others are shown in ***Figure. S1*** in the *Supplementary Material*). The fitting curves are in good agreement with the experimental data, and the distributions of the Bragg reflection are consistent with the index peaks.

Table 1. Lattice parameters obtained from Rietveld refinement for $Mg_{2-x}Cu_xAl_4Si_5O_{18}$ ($0 \le x \le 0.16$) ceramics

	$x = 0$	$x = 0.04$	$x = 0.08$	$x = 0.12$	$x = 0.16$
a (Å)	17.032(5)	17.029	17.021(4)	17.009 (5)	17.001(6)
b (Å)	9.743(20)	9.7423	9.741(20)	9.745(3)	9.746(3)
c (Å)	9.335(17)	9.338	9.332(15)	9.335(20)	9.335(20)
Vol ($Å^3$)	1548.965(0.064)	1549.280(0.000)	1547.131(0.058)	1547.313(0.069)	1546.930(0.076)
R_p(%)	10.70	9.79	11.00	11.10	12.90
R_{wp}(%)	12.60	11.30	12.20	12.20	14.10
R_{exp}(%)	6.91	7.15	6.99	6.95	7.14
χ^2	3.33	2.51	3.06	3.07	3.89

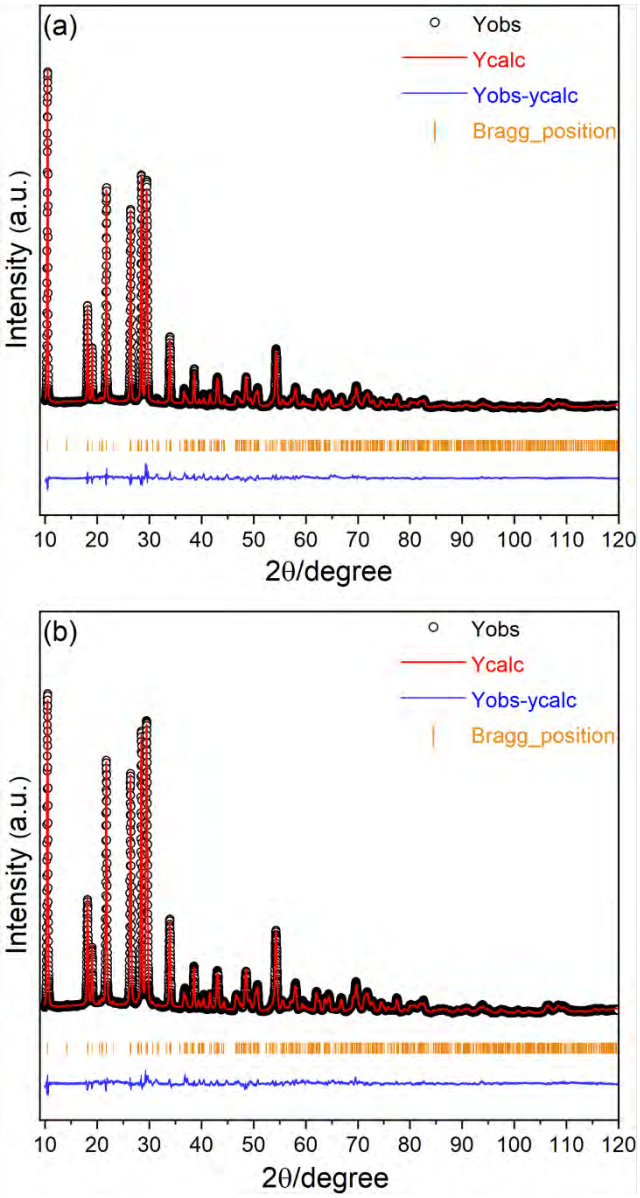

Figure 2. Rietveld refinements of samples at (a) $x = 0$ and (b) $x = 0.04$

In addition, **Figure. 3** shows the XPS spectra of the 2p orbital of Cu element peak of the $Mg_{2-x}Cu_xAl_4Si_5O_{18}$ ($x = 0.04$) ceramics sintered at 1420 °C. The Cu^{2+} can be resolved into two peaks at the binding energy values of 935.25 ($2p_{3/2}$) and 954.90 eV ($2p_{1/2}$), while the binding energy values of 933.77($2p_{3/2}$) and 953.74 eV ($2p_{1/2}$) attributed to Cu^{+}[29]. The XPS spectra results confirmed the existence of Cu^{2+} and Cu^{+}.

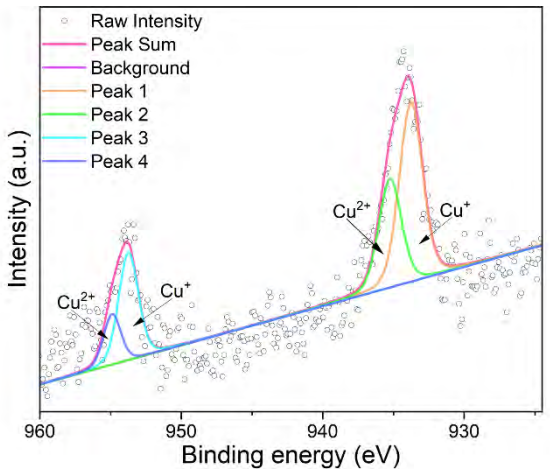

Figure 3. The Cu-2p XPS spectra of $Mg_{2-x}Cu_xAl_4Si_5O_{18}$ (x = 0.04) ceramic sintered at 1420 ℃

The EDS elemental mapping (a-e) and microanalysis data (f) of $Mg_{2-x}Cu_xAl_4Si_5O_{18}$ (x=0.04) ceramics sintered at 1420 ℃ are presented in **Figure. 4.** It clearly shows the uniform present of all elements (Mg, Al, Si, O and Cu). The EDS analysis confirmed the presence of Cu in the prepared samples. The Mg/Cu/Al/Si elements with a molar ratio of 1.96: 0.04: 4: 5 is detected in the prepared sample, which is in good agreement with the atomic ratio (Mg: Cu: Al: Si = 1.96: 0.11: 4.53: 6.11) of the selected area 1. The error between theoretical and measured results attribute to the randomly selected area.

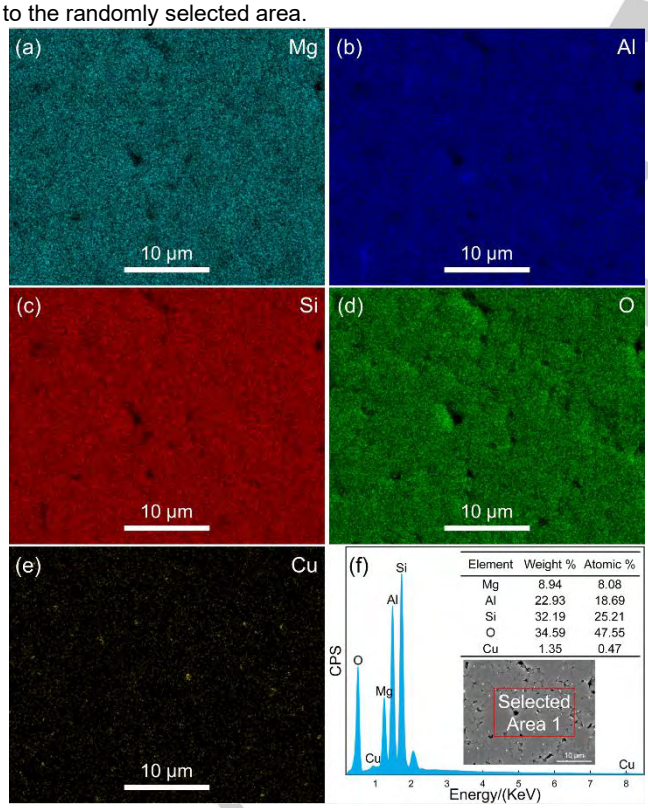

Figure 4. The EDS elemental mapping (a-e) and spectrum data of area 1 (weight and atomic percentage of elements) (f) for $Mg_{2-x}Cu_xAl_4Si_5O_{18}$ (x = 0.04) ceramic sintered at 1420 ℃

The SEM images for the $Mg_{2-x}Cu_xAl_4Si_5O_{18}$ ceramics are shown in **Figure. 5**. **Figure. 5** (a, b, c) presents the $Mg_{2-x}Cu_xAl_4Si_5O_{18}$ ($0 \le x \le 0.12$) ceramics sintered at 1420 °C. The results indicated that a moderate amount of Cu^{2+} substitution could significantly promote grain growth of the ceramics, but overabundant Cu^{2+} result in the appearance of liquid phase at the grain boundary. It also indirectly proves that CuO can reduce sintering temperature. **Figure. 5** (b, d, e, f) shows the $Mg_{2-x}Cu_xAl_4Si_5O_{18}$ (x = 0.04) ceramics that were sintered at 1400-1440 ℃ , respectively. Compared with sintering at 1400-1420 ℃ , it occurs the decrement of pores due to higher sintering temperatures (1440 ℃). Additionally, the grains become irregular when the sintering temperature exceeds 1430 ℃ . Apparently, among the SEM micrographs mentioned above, **Figure. 5** (b) has dense microstructures with less pores and uniform grain dimensions distribution.

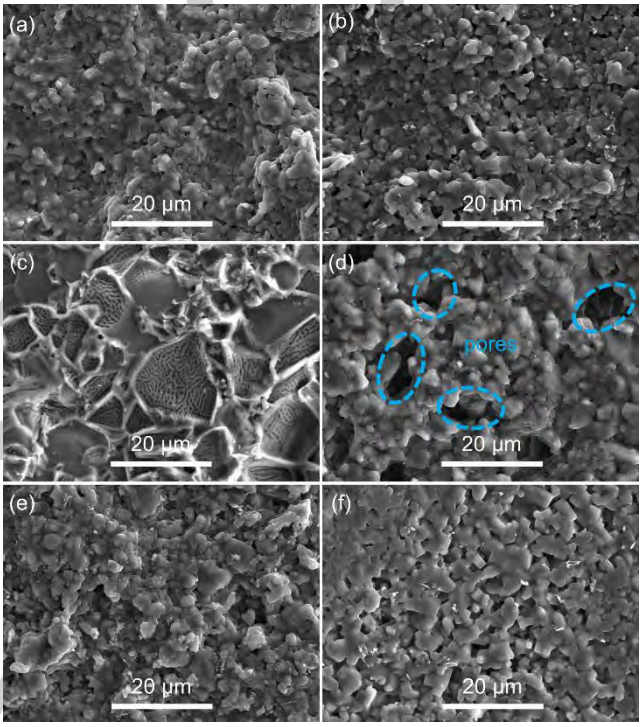

Figure 5. The SEM micrographs of $Mg_{2-x}Cu_xAl_4Si_5O_{18}$ ($0 \le x \le 0.16$) ceramics (a) x = 0, (b) x = 0.04, (c) x = 0.12 sintered at 1420 ℃ , and x = 0.04 sintered at (d) 1400 ℃ , (e) 1430 ℃ , (f) 1440 ℃

Figure. 6 (a) shows the ε_r value of the $Mg_{2-x}Cu_xAl_4Si_5O_{18}$ ($0 \le x \le 0.16$) ceramics sintered at different temperature for 4 h. With the increase in x value, the ε_r values increase at 1400 – 1410 ℃ and decrease at 1430 ℃ ; while the ε_r values first increase and then decrease after the content is higher 0.04 at 1420 ℃ . The ε_r values are generally affected by both internal and external factors. The internal factors are mainly ionic polarizability and structural characteristics, and the external factors are generally the secondary phase and densification[30]. The variation of ε_r values is affected by the microstructure presented in **Figure 5.** (a, b and c). In addition, some secondary phases, which have a significant effect on the ε_r values of the samples, were found in the XRD analysis. The secondary phases are $MgAl_2O_4$ (ε_r = 8.75)[31] at x = 0-0.08 and Al_2SiO_5 (ε_r = 4.43)[32] at $x \geqslant 0.12$, respectively. Thus, it can be concluded that the permittivity of $Mg_{2-x}Cu_xAl_4Si_5O_{18}$ ($0 \le x \le 0.08$) ceramics gradually increase under the influence of $MgAl_2O_4$ phase[33]. Moreover, the secondary phase, Al_2SiO_5, with a relatively low ε_r emerges at $x \geq 0.12$[32], and it also causes the decrease in ε_r values of the samples. The relationship between the dielectric constant (ε_r)

and the theoretical dielectric constant (ε_{theo}) are shown in **Figure. 6** (b). The equation for calculating the ionic polarizability of $Mg_{2-x}Cu_xAl_4Si_5O_{18}$ uses the Shannon additive rule as follows[30]:

$$\alpha_{theo}(Mg_{2-x}Cu_xAl_4Si_5O_{18}) = (2-x)\alpha(Mg^{2+}) + x\alpha(Cu^{2+}) + 4\alpha(Al^{3+}) + 5\alpha(Si^{4+}) + 18\alpha(O^{2-}) \quad (1)$$

where $\alpha(Mg^{2+})$ = 1.32 Å^3, $\alpha(Cu^{2+})$ = 2.11 Å^3, $\alpha(Al^{3+})$ = 0.79 Å^3, $\alpha(Si^{4+})$ = 0.87 Å^3, $\alpha(O^{2-})$ = 2.01 Å^3[30].

The theoretical dielectric constant is calculated by the Clausius-Mossotti equation[34]:

$$\varepsilon_{theo} = \frac{3V_m + 8\pi\alpha_{theo}}{3V_m - 4\pi\alpha_{theo}} \quad (2)$$

where α_{theo} and V_m are the ionic polarizability values and the molecular volume, respectively. The trend of ε_r is in agreement with ε_{theo} at x = 0-0.04 in that the polarizability is stronger for the Cu^{2+} ion[6]. Based on the above analysis, the microstructure, secondary phase and ionic polarizability are the principal factors to affect the ε_r values.

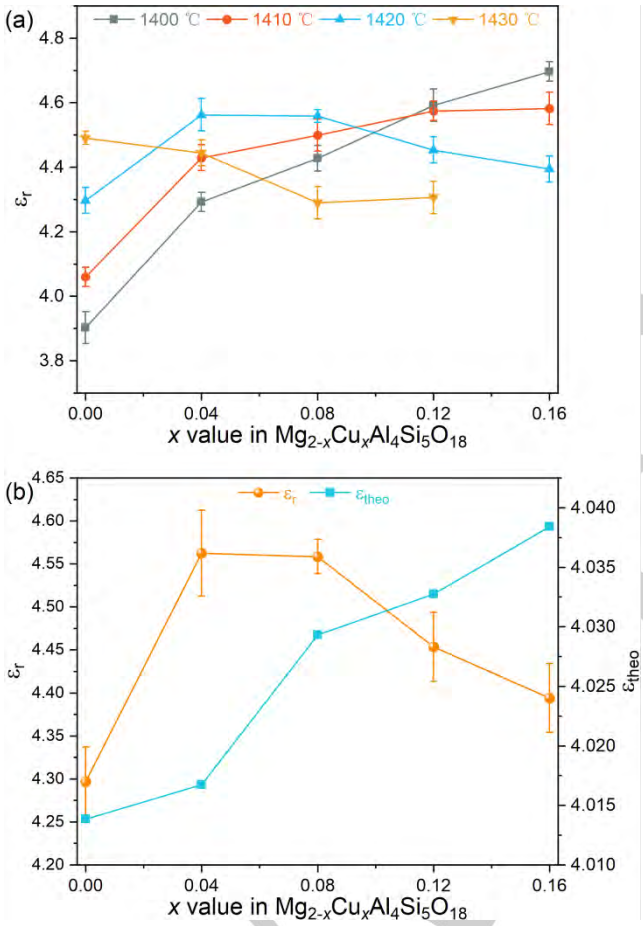

Figure 6. (a) the ε_r values of $Mg_{2-x}Cu_xAl_4Si_5O_{18}$ (0 ≤ x ≤ 0.16) ceramics sintered at different temperatures and (b) The relationship between the dielectric constant (ε_r) and the theoretical dielectric constant (ε_{theo})

Figure 7. (a) shows the Qf value of the $Mg_{2-x}Cu_xAl_4Si_5O_{18}$ ceramics at different sintered temperature. With the increase of x, the Qf values are found to increase first and then decrease. Except at x = 0.12-0.16, 1420 ℃ , the Qf values increase slightly. In general, the Qf value is a significant parameter for dielectric ceramics applications. And it is dominated by secondary phases, microstructural characteristics, centro-symmetry of hexagonal ring and the packing fraction[35,36]. Compare with x = 0-0.04, the appearance of liquid phase result in the decrease of Qf values at x ≥ 0.12 from SEM images (**Figure. 5** (a, b, c))[4,37]. According to XRD pattern (**Figure. 1**), the secondary phases are $MgAl_2O_4$ (0 ≤ x ≤ 0.08) and Al_2SiO_5 (0.08 < x ≤ 0.16). The Qf values exhibit the decreasing trend, because the Qf values of $MgAl_2O_4$ (Qf ~ 68,900 GHz)[31] are higher than that of Al_2SiO_5 (Qf ~ 41,800 GHz)[32]. Additionally, based on the previous studies[12,18], the standard deviation decreases with the increment of Qf value. Namely, the rings of $Mg_{2-x}Cu_xAl_4Si_5O_{18}$ approach to equilateral hexagonal rings, which will improve the Qf value. The standard deviation is obtained by the following equation:

$$\sigma = \sqrt{\frac{\left[\left(A_1 - 120^\circ\right)^2 + \left(A_2 - 120^\circ\right)^2 + \left(A_3 - 120^\circ\right)^2\right] \times 2}{6}} \quad (3)$$

where A_1, A_2 and A_3 are the angle of [O_6] and [Si_4Al_2] rings, respectively.

Table. S1 (*Supplementary Material*) shows the bond angle of O4-O5-O6, O5-O6-O4, O6-O4-O5, Al2-Si3-Si2, Si3-Si2-Al2, Si2-Al2-Si3. ***Figure. S2*** (*Supplementary Material*) presents the crystal structure of the sample. **Figure. 7** (b) shows the relationship between the Qf value and the standard deviation (σ) of $Mg_{2-x}Cu_xAl_4Si_5O_{18}$ (0 ≤ x ≤ 0.16) ceramics sintered at 1420 ℃ . The [Si_4Al_2] ring and Qf value are the inverse relation at x = 0-0.04 and 0.08-0.16. The result shows that the centro-symmetry of [Si_4Al_2] hexagonal ring is one of the important factors affecting the Qf value. Additionally, the effecting Qf values may include the packing fraction (pf). The packing fraction can be obtained by equation[38]:

$$\begin{aligned} Packing\ fraction(\%) &= \frac{Volume\ of\ packed\ ions}{Volume\ of\ primitive\ unit\ cell} \\ &= \frac{Volume\ of\ packed\ ions}{Volume\ of\ unit\ cell} \times Z \\ &= \frac{((2-x)r_{Mg}^3 + xr_{Cu}^3 + 4r_{Al}^3 + 5r_{Si}^3 + 18r_O^3) \times \frac{4\pi}{3}}{Volume\ of\ unit\ cell} \times Z \end{aligned} \quad (4)$$

where r_i is the ionic radius at each coordination number, and $r_{Mg^{2+}}$ = 0.72 Å, $r_{Cu^{2+}}$ = 0.73 Å, $r_{Al^{3+}}$ = 0.39 Å, $r_{Si^{4+}}$ = 0.26 Å, $r_{O^{2-}}$ = 1.38 Å. The unit cell volume is the crystal cell volume obtained by the refinement. Z = 4 is the number of formula unit cells for a cordierite compound. Liao et al.[39] reported that the packing fraction enhanced lead to reduce the lattice vibration, the Qf value improves accordingly. Namely, there is a positive correlation between Qf value and packing fraction. **Table. 2** shows the relationship between the Qf value and packing fraction of $Mg_{2-x}Cu_xAl_4Si_5O_{18}$ (0 ≤ x ≤ 0.16) ceramics sintered at 1420 ℃ , while their trends are only consistent at x ≥ 0.12. In this work, it implies that the Qf value is mainly affected by microstructure, secondary phase and centro-symmetry of [Si_4Al_2] hexagonal ring.

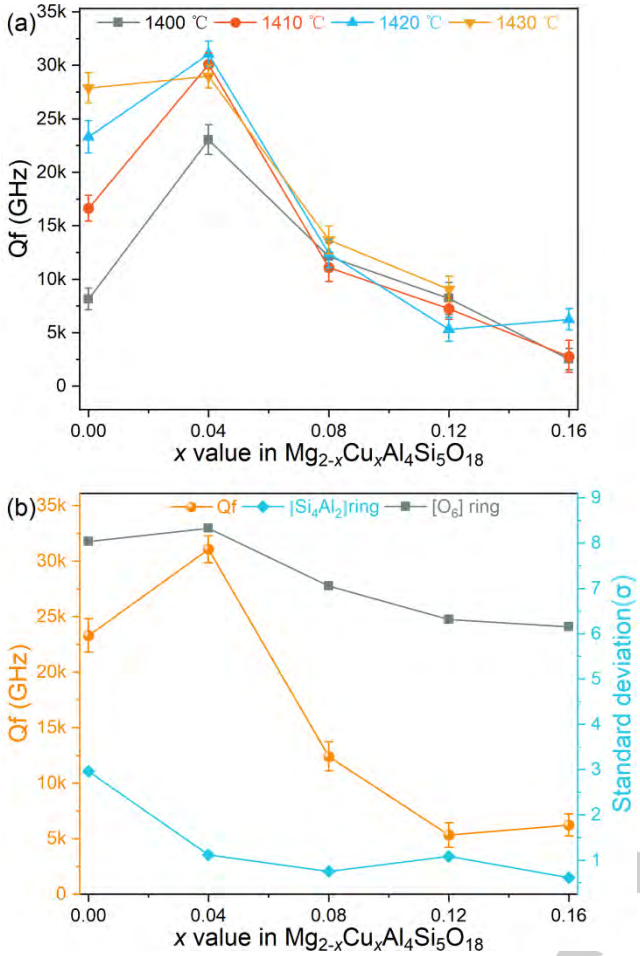

Figure 7. (a) the Qf values of $Mg_{2-x}Cu_xAl_4Si_5O_{18}$ ($0 \le x \le 0.16$) ceramics sintered at different temperatures and (b) the relationship between Qf values and standard deviation (σ) sintered at 1420 ℃

Figure. 8 (a) presents the τ_f values of the $Mg_{2-x}Cu_xAl_4Si_5O_{18}$ ceramics with various sintered temperature. In the **Figure. 8** (a), the τ_f values decrease with the increasing of x at 1410 ℃ and 1430 ℃ . The τ_f values fluctuated between -46 ppm/°C and -60 ppm/°C with the increase of Cu^{2+} content at 1420 ℃ . Generally speaking, the τ_f value is mainly influenced of oxygen band valance. The bond valance can be described as follows[40]:

$$V_i = \sum_j v_{ij} \quad (5)$$

$$v_{ij} = \exp\left(\frac{R_{ij} - d_{ij}}{b}\right) \quad (6)$$

where R_{ij}, d_{ij}, b are bond valence parameter ($R_{Mg\text{-}O}$ = 1.693 Å^3, $R_{Cu\text{-}O}$ = 1.679 Å^3), bond length and the universal constant (0.37 Å^3) [40], respectively. The bond valance parameter of Mg/Cu-O shown in **Table. 2**. The relationship between τ_f value and band valance sintered at 1420 ℃ shown in **Figure. 8** (b) which exhibits an inverse relationship. The τ_f values are associated with the oxygen bond valance, and the increase in oxygen bond valance lead to a decrease in the τ_f values[38,41,42].

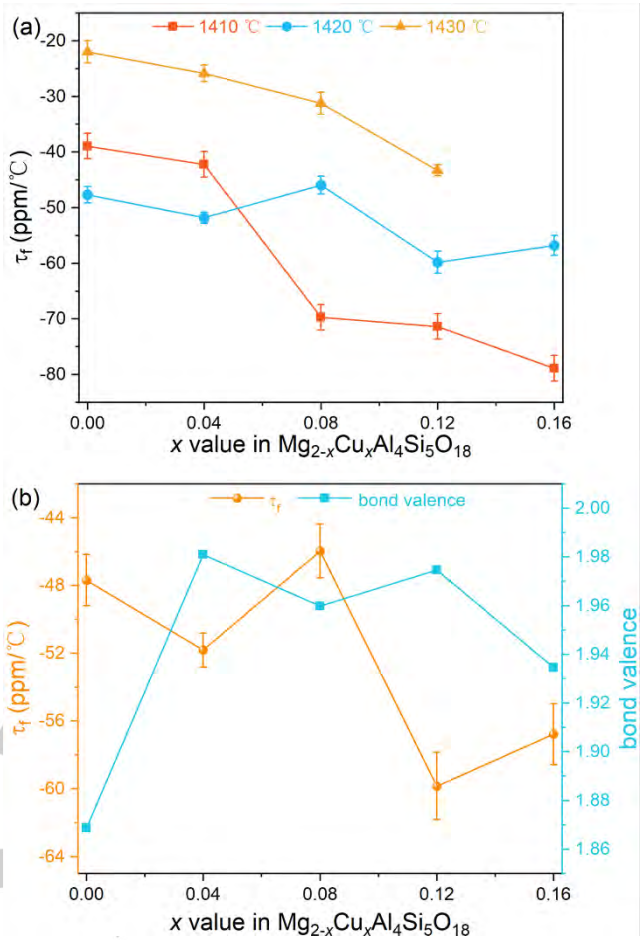

Figure 8. (a) the τ_f values of $Mg_{2-x}Cu_xAl_4Si_5O_{18}$ ($0 \le x \le 0.16$) ceramics sintered at different temperatures and (b) the relationship between τ_f values and bond valance sintered at 1420 ℃

Table 2. The Mg/Cu-O bond valance and packing fraction parameters of $Mg_{2-x}Cu_xAl_4Si_5O_{18}$ (x = 0.04) ceramics

	x = 0	x = 0.04	x = 0.08	x = 0.12	x = 0.16
$R_{Mg/Cu\text{-}O}$ (Å)	1.693	1.693	1.692	1.692	1.692
$d_{Mg/Cu\text{-}O}$ (Å)	2.125	2.103	2.106	2.103	2.111
b (Å)	0.37	0.37	0.37	0.37	0.37
$V_{Mg/Cu\text{-}O}$	1.869	1.981	1.960	1.975	1.935
Pf (%)	52.329	52.319	52.393	52.387	52.401

Generally, the high Qf decreases at the expense of high ε_r, that is, the low ε_r value is often accompanied by the poor Qf. In the practical application, it needs to solve an important issue that maintaining the balance between ε_r and Qf. **Table. 3** shows the comparison of pure $Mg_2Al_4Si_5O_{18}$ and $Mg_{2-x}Cu_xAl_4Si_5O_{18}$ (x = 0.04) with other reported cordierite. It can be seen form **Table. 3** that $Mg_{2-x}Cu_xAl_4Si_5O_{18}$ (x = 0.04) ceramic has relatively lower ε_r (~4.56) and higher Qf (~31,100) which is superior to other reported dielectric ceramics.

Table 3. The microwave dielectric properties of this wok and other reported cordierite

composition	sintering	ε_r	Qf	τ_f	Refs

	temperature (°C)		(GHz)	(ppm/°C)	.
$Mg_2Al_4Si_5O_{18}$	1420	4.30	23297	-49	This work
$Mg_{1.96}Cu_{0.04}Al_4Si_5O_{18}$	1420	4.56	31,100	-52	This work
$Mg_2Al_4Si5O_{18}$ + 30 wt.% $BaCu(B_2O_5)$	900	3.4	21,344	-30	[19]
$Mg_{1.98}(Li_{0.5}Ga_{0.5})_{0.02}Al_4Si_5O_{18}$	1375	4.72	42,170	-29	[15]
$Mg_2Al_4Si_5O_{18}$ + 50 wt.% Mg_2SiO_4	1340	5.73	76,374	-24	[20]
$(Mg_{0.9}Ni_{0.1})_2Al_4Si_5O_{18}$	1390-1440	6.2	99,110	-31	[12]
$0.9Mg_2Al_4Si_5O_{18}$ + $0.1TiO_2$	1400	6.3	55,400	-21	[17]
$0.9Mg_2Al_4Si_5O_{18}$ + $0.1SrTiO_3$	1350	6.53	80,600	-18	[18]
$0.5Mg_2Al_4Si_5O_{18}$ + $0.5CaTiO_3$	1400	7.2	55,490	-28.3	[16]

Conclusion

In summary, the $Mg_{2-x}Cu_xAl_4Si_5O_{18}$ ($0 \le x \le 0.16$) ceramics were synthesized by solid-state reaction at sintering temperature from 1400 ℃ to 1430 ℃ for 4 h. It improves the microwave dielectric properties with the substitutions of Cu^{2+} for Mg^{2+}. The microwave dielectric properties (ε_r, Qf and τ_f) of the $Mg_{2-x}Cu_xAl_4Si_5O_{18}$ ceramics were dominated by the microstructure, secondary phase, centro-symmetry of $[Si_4Al_2]$ hexagonal ring and Mg/Cu-O bond valance. The outstanding microwave dielectric properties of ε_r = 4.56, Qf = 31,100 GHz and τ_f = −52 ppm/°C were achieved at x = 0.04 sintered at 1420 ℃. In future research, more research is needed to improve the τ_f values.

Experimental Section

$Mg_{2-x}Cu_xAl_4Si_5O_{18}$ (x = 0, 0.04, 0.08, 0.12 and 0.16) ceramics were synthesized via the solid-state reaction route. According to the calculated stoichiometric proportion, analytically pure MgO (98.00%), SiO_2 (99.00%), Al_2O_3 (99.00%) and CuO (99.00%) served as raw materials (Sinopharm Chemical Reagent Co., Ltd) (the stoichiometric proportion provided in ***Table. S2*** in the ***Supplementary material***). Then the powder was milled for 4 h in plastic jars with deionized water and zirconia balls. The slurry was dried and ground into powders. Then the powers were calcined at 1350 ℃ for 4 h. The calcined powders were ball milled and dried again. Then the powders with the suitable amount of PVA solution (10 wt%) were well ground into fine particles (0.125-0.45 mm). Subsequently the particles were pressed into cylindrical disks of 12 mm diameter and 5–6 mm thickness in 10 MPa. The samples were sintered at temperatures ranging from 1400 ℃ to 1430 ℃ for 4 h in air.

The X-ray powder diffraction (XRD Miniflex600, Rigaku, Japan) was used to identify phase and structural analysis in the range of 2θ angle from 10° to 120°, the step length was 0.02°, and the time per step was 1.0 s. The FullProf software was used to refine the structure through the Rietveld method. The Scan electron microscope (SEM JSM-6490; JEOL, Japan)) was used to analyze the microstructure of sintered samples at an accelerating voltage of 20 kV. The Cu valence of prepared sample was investigated with the X-ray photoelectron spectroscopy (XPS) (XPS Nexsa, Thermo Fisher, American). The chemical elements were obtained by using the energy dispersive spectroscopy (EDS) mapping. The microwave dielectric properties (ε_r, *Qf,* τ_f) of the samples were determined by Hakki-Coleman cavity method, which were measured by Vector Network Analyzer (N5230, Agilent Technologies, USA) in the frequency ranging 10–16 GHz with a TE011 resonant peak. The τ_f values were calculated by formula[43]:

$$\tau_f = \frac{f(85°C) - f(25°C)}{f(25°C) \times (85°C - 25°C)} \quad (7)$$

where $f(85\,℃)$ and $f(25\,℃)$ represent the resonant frequency at the testing temperature of 85 ℃ and 25 ℃, respectively.

Acknowledgements

This work was supported by the fund of the State Key Laboratory of Advanced Technologies for Comprehensive Utilization of Platinum Metals under Grant No. SKL-SPM-202021. The scientific research launching funds from Chengdu University of Technology under Grant No.KYQD2019_07728.

10.1002/ejic.202100174

Keywords: Microwave dielectric ceramic • Cordierite • Structure • millimeter-wave communication

[1] H. J. Wang, T. Zscheckel, H. X. Lin, B. T. Li, C. Rüssel, L. Luo, *Ceram. Int.* **2017**, *43*, 7073-7079.

[2] L. X. Pang, D. Zhou, W. B. Li, Z. X. Yue, *J. Eur. Ceram. Soc.* **2017**, *37*, 3073-3077.

[3] R. Naveenraj, E. K. Suresh, J. Dhanya, R. Ratheesh, *Eur. J. Inorg. Chem.* **2019**, *7*, 949-955.

[4] C. Zhang, R. Zuo, J. Zhang, Y. Wang, *J. Am. Ceram. Soc.* **2015**, 98, 702–*710*.

[5] Y. Guo, H. Ohsato, K. Kakimoto, *J. Eur. Ceram. Soc.* **2006**, *26*, 1827-1830.

[6] Y. Lai, X. Tang, X. Huang, H. Zhang, X. Liang, J. Li, H. Su, *J. Eur. Ceram. Soc.* **2018**, 38, 1508–1516.

[7] X. Huang, H. Zhang, Y. Lai, G. Wang, M. Li, C. Hong, J. Li, *Eur. J. Inorg. Chem.* **2018**, *17*, 1800-1804.

[8] H. Ohsato, I. Kagomiya, M. Terada, K. Kakimoto, *J. Eur. Ceram. Soc.* **2010**, *30*, 315-318.

[9] C. Tseng, P. Tsai, *Ceram. Int.* **2013**, *39*, 75-79.

[10] S. B. Narang, S. Bahel, *J. CERAM. PROCESS. RES.* **2010**, 11, 316-321.

[11] T. Okamura, T. Kishino, *Jpn. J. Appl. Phys.* **1998**, *37*, 5364-5366.

[12] M. Terada, K. Kawamura, I. Kagomiya, K. ichi Kakimoto, H. Ohsato, *J. Eur. Ceram. Soc.* **2007**, *27*, 3045-3048.

[13] H. Ikawa, T. Otagiri, O. Imai, M. Suzuki, K. Urabe, *Appl. Ph.* **1986**, *69*, 492-498.

[14] H. Ohsato, J. S. Kim, A. Y. Kim, C. Il Cheon, K. W. Chae, *Jpn. J.ys.* **2011**, *50*, 09NF01.

[15] W. Lou, K. Song, F. Hussain, B. Liu, H. B. Bafrooei, H. Lin, W. Su, F. Shi, D. Wang, *Ceram. Int.* **2020**, *46*, 28631-28638.

[16] J. Wei, P. Liu, H. Lin, Z. Ying, P. Zheng, W. Su, K. Song, H. Qin, *J. Alloys Compd.* **2016**, *689*, 81-86.

[17] S. Wu, K. Song, P. Liu, H. Lin, F. Zhang, P. Zheng, H. Qin, *J. Am. Ceram. Soc.* **2015**, *98*, 1842-1847.

[18] K. Song, S. Wu, P. Liu, H. Lin, Z. Ying, P. Zheng, W. Su, J. Deng, L. Zheng, H. Qin, *J. Alloys Compd.* **2015**, *628*, 57-62.

[19] J. Deng, H. Zhou, S. Li, C. Lu, K. Wang, W. Sun, *J. Electron. Mater.* **2020**, *49*, 1184-1188.

[20] X. Dong, C. Sun, H. Yang, L. Yang, S. Zhang, *J. Mater. Sci. Mater. Electron.* **2018**, *29*, 17967-17973.

[21] C. L. Huang, M. H. Weng, *Mater. Res. Bull.* **2000**, *35*, 1881-1888.

[22] D. W. Kim, K. H. Ko, K. S. Hong, *J. Am. Ceram. Soc.* **2001**, *84*, 1286-1290.

[23] C. F. Tseng, *J. Alloys Compd.* **2010**, *494*, 252-255.

[24] J. J. Wang, C. H. Hsu, C. L. Huang, R. J. Lin, *Jpn. J. Appl. Phys.* **2005**, *44*, 8039-8042.

[25] Y. Lai, X. Tang, H. Zhang, X. Liang, X. Huang, Y. Li, H. Su, *Mater. Res. Bull.* **2018**, *99*, 496-502.

[26] Y. Lai, Y. Zeng, J. Han, X. Liang, M. Liu, B. Duo, H. Su, *J. Eur. Ceram. Soc.* **2020**, *99*, 2602-2609.

[27] Y. Lai, H. Su, G. Wang, X. Tang, X. Liang, X. Huang, Y. Li, H. Zhang, C. Ye, X. R. Wang, *J. Alloys Compd.* **2019**, *772*, 40-48.

[28] J. Rodríguez-Carvajal, *Phys. B Phys. Condens. Matter.* **1993**, *192*, 55-69.

[29] Q. Zhang, S. Wen, Q. Feng, J. Liu, *Appl. Surf. Sci.* **2021**, *543*, 148795-148803.

[30] R. D. Shannon, F. L. D. Shannon, J. Appl. Phys. **1993**, *73*, 348-366.

[31] K. P. Surendran, P. V. Bijumon, P. Mohanan, M. T. Sebastian, *Appl. Phys. A Mater. Sci. Process.* **2005**, *81*, 823-826.

[32] I. J. Induja, M. T. Sebastian, *J. Eur. Ceram. Soc.* **2017**, *37*, 2143-2147.

[33] S. Takahashi, A. Kan, H. Ogawa, *Mater. Chem. Phys.* **2017**, *200*, 257-263.

[34] W. Lei, W. Lu, D. Liu, J. Zhu, *J. Am. Ceram. Soc.* **2009**, *92*, 105-109.

[35] S. D. Ramarao, V. R. K. Murthy, *Scr. Mater.* **2013**, *69*, 274-277.

[36] S. Roopas Kiran, G. Sreenivasulu, V. R. K. Murthy, V. Subramanian, B. S. Murty, *J. Am. Ceram. Soc.* **2012**, *95*, 6963-6969.

[37] Y. J. Eoh, H. J. Ahn, E. S. Kim, *Ceram. Int.* **2015**, *41*, S544-S550.

[38] E. S. Kim, B. S. Chun, R. Freer, R. J. Cernik, *J. Eur. Ceram. Soc.* **2010**, *30*, 1731-1736.

[39] D. A. Links, Q. Liao, L. Li, *Dalton Trans.* **2012**, *41*, 6963-6969.

[40] N. E. Brese, M. O'Keeffe, *Acta Crystallogr. Sect. B.* **1991**, *47*, 192-197.

[41] T. Qin, C. Zhong, Y. Qin, B. Tang, S. Zhang, *Ceram. Int.* **2020**, *46*, 19046-19051.

[42] H. S. Park, K. H. Yoon, E. S. Kim, *J. Am. Ceram. Soc.* **2001**, *84*, 99-103.

[43] B. W. Hakki, P. D. Coleman, *IRE Trans. Microw. Theory Tech.* **1960**, *MTT-8*, 402-410.

Entry for the Table of Contents

The $Mg_{2-x}Cu_xAl_4Si_5O_{18}$ ($0 \leq x \leq 0.16$) ceramics were synthesized by solid-state reaction at sintering temperature from 1400 ℃ to 1430 ℃ for 4 h. It improves the microwave dielectric properties (ε_r, Qf and τ_f) with the substitutions of Cu^{2+} for Mg^{2+}. In comparison to pure $Mg_2Al_4Si_5O_{18}$ ceramics, the excellent microwave dielectric properties with ε_r = 4.56, Qf = 31,100 GHz and τ_f = −52 ppm/°C were obtained at x = 0.04 with sintering at 1420 ℃ . Thus, the $Mg_{2-x}Cu_xAl_4Si_5O_{18}$ ($0 \leq x \leq 0.16$) ceramics will be promising millimeter-wave communication materials.